J|A|C|S
ARTICLES

Published on Web 08/13/2010

Spontaneous and Specific Activation of Chemical Bonds in Macromolecular Fluids

Insun Park,[†] David Shirvanyants,[†] Alper Nese,[‡] Krzysztof Matyjaszewski,[‡] Michael Rubinstein,[†] and Sergei S. Sheiko*,[†]

Department of Chemistry, University of North Carolina at Chapel Hill, Chapel Hill, North Carolina 27599-3290, and Department of Chemistry, Carnegie Mellon University, 4400 Fifth Avenue, Pittsburgh, Pennsylvania 15213

Received July 4, 2010; E-mail: sergei@email.unc.edu

Abstract: Mechanical activation of chemical bonds typically involves the application of external forces, which implies a broad distribution of bond tensions. We demonstrate that controlling the flow profile of a macromolecular fluid generates and delineates mechanical force concentration, enabling a hierarchical activation of chemical bonds on different length scales from the macroscopic to the molecular. Bond tension is spontaneously generated within brushlike macromolecules as they spread on a solid substrate. The molecular architecture creates an uneven distribution of tension in the covalent bonds, leading to spatially controlled bond scission. By controlling the flow rate and the gradient of the film pressure, one can sever the flowing macromolecules with high precision. Specific chemical bonds are activated within distinct macromolecules located in a defined area of a thin film. Furthermore, the flow-controlled loading rate enables quantitative analysis of the bond activation parameters.

Introduction

Mechanical activation of chemical bonds plays a vital role in biology, chemistry, and materials engineering.[1−4] Along with other activation stimuli such as light, heat, and an electric field, mechanical forces control metabolism of cells, trigger chemical reactions, and induce color changes of materials.[5−16] However, such forces are usually generated by external stimuli such as ultrasonic waves, hydrodynamic flow, and mechanical deformations that offer limited means for control at the molecular scale, e.g., for activating individual chemical bonds. Force generation and accurate control of mechanical tension in covalent bonds is very challenging, but this can be accomplished by designing interactive molecules that respond to changes in the environment. Here, we demonstrate a system which generates, amplifies, and transmits mechanical tension to specific chemical bonds. The set of strained bonds emerges during spreading of brushlike macromolecules on a substrate, and the bond tension exhibits a fast response to minute variations in the film pressure. The extraordinary sensitivity of chemical bonds to mechanical stresses in thin films has direct implications for spreading of biological cells, biochemical sensors, and heterogeneous catalysis.

Similar to other flow processes,[17−19] spreading causes extension of polymer chains. However, the origin of chain extension in thin films is different from the elongational flow in bulk fluids. In spreading films, extension of macromolecules occurs due to progressive adsorption of chain segments as the film pressure reduces along the flow direction.[20] The effect of adsorption is amplified in branched macromolecules, such as stars, dendrimers, and brushes.[21] Steric repulsion between the densely packed branches raises the tension from the 10 pN to 1 nN level, triggering scission of strong covalent bonds.[22] The spreading-induced molecular fracture has two distinct features. First, it occurs spontaneously driven by minimization of the surface free

[†] University of North Carolina at Chapel Hill.
[‡] Carnegie Mellon University.

(1) Bensimon, D. *Structure (London)* **1996**, *4*, 885–889.
(2) Evans, E. *Annu. Rev. Biophys. Biomol. Struct.* **2001**, *30*, 105–128.
(3) Beyer, M. K.; Clausen-Schaumann, H. *Chem. Rev.* **2005**, *105*, 2921–2948.
(4) Caruso, M. M.; Davis, D. A.; Shen, Q.; Odom, S. A.; Sottos, N. R.; White, S. R.; Moore, J. S. *Chem. Rev.* **2009**, *109*, 5755–5798.
(5) Discher, D. E.; Janmey, P.; Wang, Y.-l. *Science* **2005**, *310*, 1139–1143.
(6) Vale, R. D.; Milligan, R. A. *Science* **2000**, *288*, 88–91.
(7) Carter, N. J.; Cross, R. A. *Nature* **2005**, *435*, 308–312.
(8) Evans, E. A.; Calderwood, D. A. *Science* **2007**, *316*, 1148–1151.
(9) Wiita, A. P.; Ainavarapu, R. K.; Huang, H. H.; Fernandez, J. M. *Proc. Natl. Acad. Sci. U.S.A.* **2006**, *103*, 7222–7227.
(10) Bhowmick, A. K.; Ray, S.; Bhowmick, A. M.; Heslop, J.; Koppen, N.; White, J. R. *J. Appl. Polym. Sci.* **2006**, *99*, 150–161.
(11) Rohrig, U. F.; Troppmann, U.; Frank, I. *Chem. Phys.* **2003**, *289*, 381–388.
(12) Hickenboth, C. R.; Moore, J. S.; White, S. R.; Sottos, N. R.; Baudry, J.; Wilson, S. R. *Nature* **2007**, *446*, 423–427.
(13) Piermattei, A.; Karthikeyan, S.; Sijbesma, R. P. *Nat. Chem.* **2009**, *1*, 133–137.
(14) Yang, Q. Z.; Huang, Z.; Kucharski, T. J.; Khvostichenko, D.; Chen, J.; Boulatov, R. *Nat. Nanotechnol.* **2009**, *4*, 302–306.
(15) Lenhardt, J. M.; Craig, S. L. *Nat. Nanotechnol.* **2009**, *4*, 284–285.
(16) Davis, D. A.; Hamilton, A.; Yang, J. L.; Cremar, L. D.; Van Gough, D.; Potisek, S. L.; Ong, M. T.; Braun, P. V.; Martinez, T. J.; White, S. R.; Moore, J. S.; Sottos, N. R. *Nature* **2009**, *459*, 68–72.
(17) Schroeder, C. M.; Babcock, H. P.; Shaqfeh, E. S.; Chu, S. *Science* **2003**, *301*, 1515–1518.
(18) Bensimon, A.; Simon, A.; Chiffaudel, A.; Croquette, V.; Heslot, F.; Bensimon, D. *Science* **1994**, *265*, 2096–2098.
(19) Odell, J. A.; Keller, A. *J. Polym. Sci., Part B* **1986**, *24*, 1889–1916.
(20) Xu, H.; Shirvaniants, D.; Rubinstein, M.; Shabratov, D.; Beers, K.; Matyjaszewski, K.; Sheiko, S. S. *Adv. Mater.* **2007**, *19*, 2930–2934.
(21) Panyukov, S.; Zhulina, E. B.; Sheiko, S. S.; Randall, G.; Brock, J.; Rubinstein, M. *J. Phys. Chem. B* **2009**, *113*, 3750–3768.
(22) Sheiko, S. S.; Sun, F. C.; Randall, A.; Shirvanyants, D.; Rubinstein, M.; Lee, H.-i.; Matyjaszewski, K. *Nature* **2006**, *440*, 191–194.

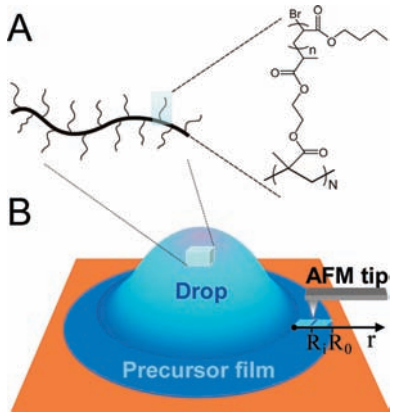

Figure 1. (A) Chemical structure of brushlike macromolecules composed of a polymethacrylate backbone and poly(*n*-butyl acrylate) side chains. (B) A drop of a polymer melt was deposited onto a mica substrate and allowed to spread under a controlled environment. The molecular structure of the precursor film was monitored by AFM along the flow direction (*r*-axis).

energy. Second, the intrinsic gradient of the film pressure creates a well-defined loading rate for each individual molecule within the flowing film, enabling quantitative analysis of bond activation. The time evolution of bond tension for molecule *i* within a spreading film of length R_0 is given by (see Supporting Information for the derivation of eq 1)

$$f_i(t) = \left(1 - \sqrt{\frac{\Delta t_i}{t + \Delta t_i}}\right) f_0 \qquad (1)$$

where f_0 is the maximum tensile force which is achieved at the film edge and Δt_i is the lag in spreading time of molecule *i* sited inside the propagating film ($r = R_i$) with respect to molecules at the film edge ($r = R_0$) that spread first (Figure 1).

Results and Discussion

Scission of Covalent Bonds during Spreading. A series of brushlike macromolecules having a long polymethacrylate (PMA) backbone with a degree of polymerization of $N = 3600$ and poly(*n*-butyl acrylate) (PBA) side chains with three different degrees of polymerization ($n = 80$, 110, 140) was prepared using atom transfer radical polymerization (Figure 1A).[23,24] As reported previously, the polymer backbone of brushlike macromolecules is under tension induced by steric repulsion between the densely grafted side chains.[21] However, in bulk melts and solutions, this tension is on the order of 10−100 pN, which may be sufficient to break relatively weak hydrogen bonds. Adsorption and spreading of molecular brushes enhance crowdedness of the side chains, which leads to amplification of the backbone tension from the piconewton to nanonewton level, exceeding the strength of a typical covalent bond. Flow-induced fracture of individual macromolecules was monitored by atomic force microscopy (AFM) as shown in Figure 1B. Molecular resolution is facilitated by the side chains that separate polymer backbones, enhance backbone stiffness, and generate height contrast through partial segregation of desorbed side chains along the backbone.[25] Parts A and B of Figure 2 show two series of height micrographs captured along the spreading direction for two different precursor films obtained upon long-time ($t_0 =$ 600 s) and short-time ($t_0 = 2$ s) spreading on mica, respectively. In both cases, one observes an abrupt decrease of the molecular size within a relatively narrow section of the film. The fracture region becomes particularly narrow in shorter films with a steeper tension gradient. For example, in a 18-μm-long film, all molecules break apart within a film region confined between $r = 14.6$ and 15.7 μm (Figure 2B). Since the width of the region ($\Delta r \cong 1$ μm) becomes comparable to the number-average length of individual macromolecules ($L_n = 760 \pm 20$ nm), molecular fragments get chopped off in a knifelike fashion at the moment a molecule enters the fracture zone. Figure 2C presents a collection of data that depict the variation in the contour length along the flow axis for different precursor films allowed to spread for different times t_0. Near the drop, the molecules maintain their original length $L_0 = 760$ nm within an extended range of distances from the drop boundary. Approximately in the middle of each film (Figure 2C), molecules undergo a rapid degradation by a factor of 20 followed by a second plateau at $L_\infty = 36$ nm.

The avalanche-like degradation of flowing macromolecules is attributed to the exponential dependence of the bond lifetime τ on the applied force *f*. After Arrhenius, Eyring, Zhurkov, and Bell,[26−28] the force dependence of the rate constant of bond scission ($k = 1/\tau$) can be described by the following phenomenological equation:

$$k = k_0 \exp\left(-\frac{E_a - f b_a}{k_B T}\right) \qquad (2)$$

where k_0 is the preexponential factor on the order of the bond oscillation frequency ($\nu_0 = k_B T/\hbar \cong 10^{13}$ s^{-1}); $E_a = E_{TS} - E_0$ is the activation energy, i.e., the height of the energy barrier between the transition state (E_{TS}) and the minimum of the bond-potential well (E_0); b_a is the activation length, i.e., the distance along the reaction coordinate from the energy minimum to the transition state. Note that the bond tension *f* and thus the rate constant *k* are time-dependent. As the tensile force progressively increases along the spreading direction (eq 1), the bond lifetime $\tau = 1/k$ drops by many orders of magnitude, prompting abrupt fracture of the flowing macromolecules. Figure 2D shows the behavior of the bond tension and the bond lifetime for two different macromolecules during their displacement from $r =$ 0 (drop boundary) to $r = 110$ μm (molecule 1) and $r = 150$ μm (molecule 2), respectively. The tension values were calculated as a product of the spreading parameter and the brush width.[22] This macroscopic calculation is consistent with the scaling analysis of a brushlike macromolecule adsorbed to a solid substrate, which predicts the force value as $f \cong SL$, where *S* is the spreading parameter and *L* is the contour length of a side chain.[21] It also important to emphasize that, due to symmetric distribution of the side chains, the force is directed along the backbone. Furthermore, the force direction is independent of the orientation of the molecules with respect to the direction of spreading, which behaves as plug flow with all species moving with the same velocity.

The corresponding loading rates (eq 1) were used to fit the measured variations of the molecular contour length *L* as a function of the distance from the drop boundary *r* using the

(23) Sheiko, S. S.; Sumerlin, B. S.; Matyjaszewski, K. *Prog. Polym. Sci.* **2008**, *33*, 759–785.
(24) Matyjaszewski, K.; Tsarevsky, N. V. *Nat. Chem.* **2009**, *1*, 276–279.
(25) Xu, H.; Sheiko, S. S.; Shirvaniants, D.; Rubinstein, M.; Beers, K. L.; Matyjaszewski, K. *Langmuir* **2006**, *22*, 1254–1259.
(26) Kauzmann, W. J.; Eyring, H. *J. Am. Chem. Soc.* **1940**, *62*, 3113–3118.
(27) Zhurkov, S. N. *Int. J. Fract. Mech.* **1965**, *1*, 311–316.
(28) Bell, G. I. *Science* **1978**, *200*, 618–627.

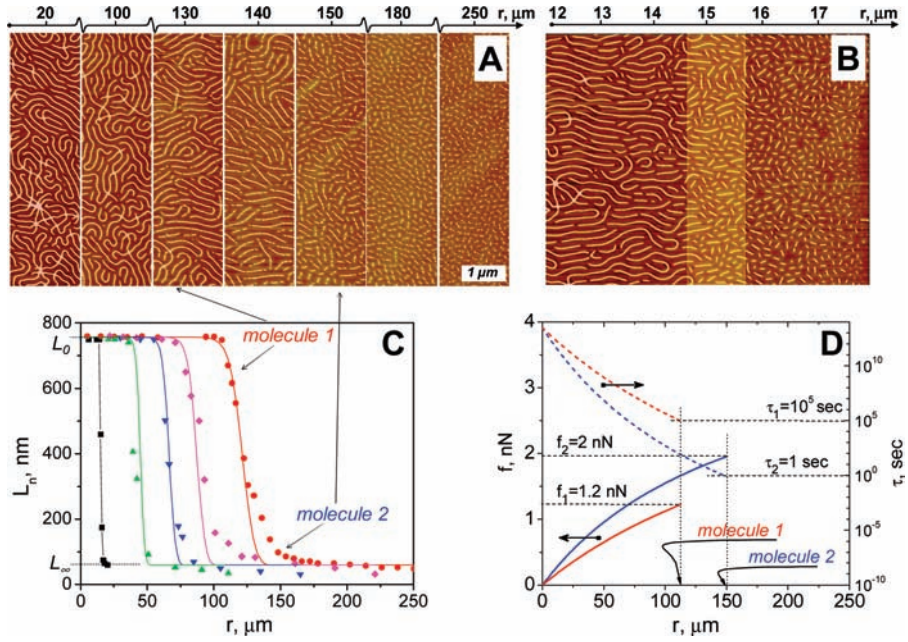

Figure 2. AFM height images of molecular brushes ($n = 140$) captured during spreading at different distances from the drop boundary within (A) long ($R_0 = 321$ μm, $t_0 = 600$ s) and (B) short ($R_0 = 18$ μm, $t_0 = 2$ s) precursor films. The flowing macromolecules fracture predominately within a narrow region (highlighted in (B)) as the bond tension reaches the nanonewton level (see (D)). (C) The number-average contour length (L_n) of the macromolecules is plotted as a function of distance from the drop for different spreading times (■, $t_0 = 2$ s; ▲, $t_0 = 70$ s; ▼, $t_0 = 180$ s; ◆, $t_0 = 300$ s; ●, $t_0 = 600$ s). All data points (collected from the different samples) have been fitted (eq 3) using a single set of two fitting parameters: activation energy and activation length (solid lines). (D) Every molecule within a spreading film has an individual loading history leading to a well-defined temporal variation of the bond tension f (solid lines) and the corresponding bond lifetime $\tau = 1/k$ (dashed lines, log scale). The plot depicts the loading history and the bond lifetime of two molecules (molecules 1 and 2) located at distances $r = 110$ μm and $r = 150$ μm from the drop boundary within a film formed after $t_s = 600$ s spreading. The approximate locations of molecules 1 and 2 are indicated by arrows in (A) and (C).

following equation (see the Supporting Information for the derivation of eq 3):

$$\ln \frac{1 - \frac{L_\infty}{L}}{1 - \frac{L_\infty}{L_0}} = -\int_0^{t_i} k(t)\, dt \qquad (3)$$

where t_i is the duration of flow for a particular molecule (molecule i) located at distance $r = R_i$ from the drop boundary; $L_0 = 750$ nm and $L_\infty = 36$ nm are the number-average contour lengths at $t = 0$ and $t = t_s$, respectively. The five solid lines in Figure 2C, which correspond to different samples prepared at different spreading times, were obtained using a single set of only two fitting parameters: the activation energy $E_a = 109$ kJ/mol and the activation length $b_a = 0.38$ Å. While the length value is consistent with the literature data,[29] the activation energy is underestimated due to preextended conformation of molecular brushes prior to spreading as discussed at the beginning of this section.

So far, it has been demonstrated that one can activate and sever strong covalent bonds within a specific area of a spreading film. The precision and specificity of the flow-induced bond scission can be further enhanced by controlling the molecular architecture. Two examples are presented below to demonstrate a proof-of-concept for (i) breaking specific molecules within a macroscopic film and (ii) breaking a specific chemical bond within a flowing macromolecule.

Breaking Specific Molecules. The first system represents a 50/50 mol/mol mixture of two brushes having different degrees of polymerization of the PBA side chains ($n = 140$ and $n = 110$) (Figure 3). The chemically identical molecules are fully miscible and hence virtually indistinguishable by AFM (left image in Figure 3B). However, the molecules reveal their identity upon breaking during the spreading process (middle image in Figure 3B). Figure 3C depicts variations of the reciprocal contour length within a precursor film as a function of distance from the drop boundary.

Plotting the data as $1/L(r)$ allows distinct resolution of the two-step degradation process resulting in spatial separation of the two fracture zones by an interval of ca. $\Delta r = 100$ μm along the flow direction. The first step at $r \cong 140$ μm corresponds to scission of the macromolecules with longer side chains ($n = 140$), which is followed by the second step at $r \cong 230$ μm due to degradation of the brushes with shorter side chains ($n = 110$). The stepwise degradation is ascribed to the increase of the backbone tension with the degree of polymerization of the side chains.[21] The bond tension within the molecules with longer side chains is a factor of ca. 140/110 ≅ 1.27 higher than for the shorter brushes. As discussed previously (Figure 2D), the fairly small difference in tension (27%) causes a significant, ca. 4 order of magnitude difference in the bond lifetime as predicted by DFT calculations.[29] The molecular identity of the mixed fluid was verified by studying the spreading behavior of one-component systems (Figure S1, Supporting Information). As shown in Figure 3C, polymer melts composed of $n = 140$ and $n = 110$ undergo degradation at different distances from the drop that are in full agreement with the locations of the two steps in the corresponding mixture. Furthermore, the location of the steps is consistent with the model's prediction (red solid line, Figure 3C) obtained by using the same fitting parameters as in Figure 2C, i.e., $E_a = 109$ kJ/mol and $b_a =$

(29) Beyer, M. K. *J. Chem. Phys.* **2000**, *112*, 7307–7312.

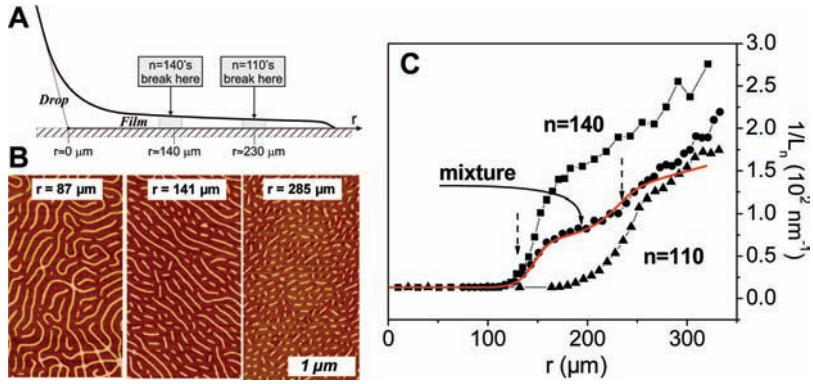

Figure 3. (A) AFM revealing that pBA brushes having the same backbone ($N = 3600$) but different side chains ($n = 140$ and 110) undergo scission at different distances from the drop (Supporting Information). (B) The site-specific scission becomes particularly clear in the height images of a binary 50/50 mol/mol mixture of $n = 140$ and 110 brushes. The height images were captured at three different distances from the drop (87, 141, and 285 μm) to demonstrate the two-step molecular degradation process. At shorter distances (e.g., $r = 87$ μm), the molecules of both types are intact. At intermediate distances around $r = 141$ μm, the molecular brushes with the longer ($n = 140$) side chains break, while their counterparts with the shorter ($n = 110$) side chains remain intact. At long distances, (e.g., $r = 285$ μm), molecules of both types undergo complete degradation. (C) The corresponding variations of the molecular contour length $1/L(r)$ depict the two-step (dashed arrows) degradation process. The stepwise degradation of the polymer mixture (●) is consistent with the onset of molecular degradation in the individual systems (■, $n = 140$, and ▲, $n = 110$; Supporting Information) and with the model prediction (red solid line).

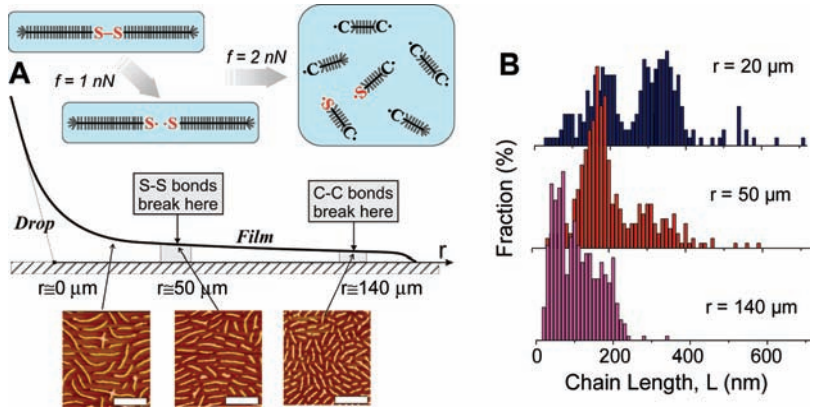

Figure 4. (A) Schematics of the degradation process of molecular brushes having a disulfide bond in the middle of the backbone. During flow, the rupture of the disulfide linker is followed by random scission of carbon−carbon bonds. The height AFM images are captured at three different distances from the drop edge ($r = 20$, 50, and 140 μm) to demonstrate the midchain S−S fracture of the brushlike macromolecules followed by the scission of the C−C bonds. (B) The histograms depict the variation of the length distribution along the spreading direction (r). At distances from 20 to 50 μm, molecular brushes undergo the midchain scission, which is followed by the random scission of C−C bonds at $r = 100-140$ μm. The S−S and C−C scission regions are spatially separated; i.e., no bond scission occurs between 50 and 100 μm.

0.38 Å. Initially, the red solid line in Figure 3C (model prediction) nearly exactly coincides with an average curve (not shown) of the two individual systems ($n = 110$ and 140). The discrepancy at larger distances from the drop (higher tension region) is due to the fact that the degradation process of shorter molecules (products of the scission process) changes its pattern from random to midchain scission, to be discussed elsewhere. With respect to polymer mixtures in flow, it is important to emphasize that the macroscopic film tension at a given distance from the drop is the same for all studied systems. However, on sub-100 nm length scales, the transduction of the macroscopic stress to chemical bonds is determined by the molecular architecture, leading to preferential scission of those macromolecules that are overstressed.

Activating Specific Bonds. In the second system, we have aimed at controlling molecular fracture on the scale of individual bonds. For this purpose, we have synthesized brushlike macromolecules with a disulfide linker in the middle of the all-carbon polymethacrylate backbone.[30] Figure 4A shows height images captured from different distances from the polymer drop along with the corresponding molecular length distributions (Figure 4B). At the beginning of spreading ($x = 20$ μm) one observes a bimodal distribution, which indicates the midchain fracture of the disulfide-containing brushes. The peaks at $L \cong 320$ nm and at $L/2 \cong 160$ nm correspond to full molecules and their halves, respectively. At larger distances from the drop, e.g., $x = 50$ μm, the fraction of the midchain fractured molecules increases at the expense of the full molecules. This corroborates that the degradation process in the low-tension areas (ca. 1 nN) is dominated by the scission of the disulfide linker ($E_{S-S} = 268$ kJ/mol) proceeding at a much faster rate compared to the stronger C−C bonds ($E_{C-C} = 347$ kJ/mol) in the same backbone. The onset of scission of the C−C bonds occurs at larger distances from the drop at 140 μm, where the bond tension reaches a magnitude of 2 nN (Figure 2D). As such, the spreading-induced tension in the polymer backbone probes the strength of individual bonds triggering scission of the weaker ones.

Conclusions

In conclusion, spreading of complex polymer fluids allows severing specific covalent bonds within branched macromol-

(30) Park, I.; Sheiko, S. S.; Nese, A.; Matyjaszewski, K. *Macromolecules* **2009**, *42*, 1805–1807.

ecules located in a defined area of macroscopic film. The bond scission does not require any external force and occurs spontaneously as the film pressure decreases along the spreading direction. The precision and selectivity of bond activation are controlled by tuning the molecular architecture, fluid composition, and flow conditions. The control parameters also include the chemical composition of the substrate, vapor pressure, boundary conditions, flow configuration, and additives to the spreading fluid. As shown in Figure S2 (Supporting Information), by adding diluents (e.g., melt of linear PBA) into the melt of polymer brushes, one can decrease the pressure gradient and thus shift the fracture zone to a longer distance from the drop. The flow-induced molecular rupture provides a new tool for quantitative analysis of the bond activation parameters. By incorporating a specific linker (e.g., disulfide bond) into the brush backbone, one effectively decouples the tension generator (brush section) and the probe (linker). Note that a single spreading process enables concurrent analysis of ca. 1000 individual molecules that have experienced different loading histories. This is a significant step forward in the experimental studies of bond activation parameters. One can also use this approach to quantify the pressure gradient using molecules with known activation parameters. The force-responsive macromolecules could inspire the intelligent design of stimuli-responsive and interactive systems for sensor, lithography, and catalytic applications.

Acknowledgment. We gratefully acknowledge funding from the National Science Foundation (DMR 0906985, CBET-0609087).

Supporting Information Available: Mathematical derivation of eqs 1 and 3, flow-induced fracture of brushlike macromolecules with different length of the side chain (Figure S1), effect of diluent on the scission rate (Figure S2), and the Experimental Section. This material is available free of charge via the Internet at http://pubs.acs.org.

JA105897B